IEEE Open Access Journal of Power and Energy

Received 29 June 2022; revised 27 September 2022 and 3 December 2022; accepted 20 December 2022.
Date of publication 26 December 2022; date of current version 12 January 2023.

Digital Object Identifier 10.1109/OAJPE.2022.3232186

A Benchmarking Testbed for Low-Voltage Active Distribution Network Studies

CHRISTOS L. ATHANASIADIS [1,2] (Student Member, IEEE), THEOFILOS A. PAPADOPOULOS [1] (Senior Member, IEEE), GEORGIOS C. KRYONIDIS [3] (Member, IEEE), AND KALLIOPI D. PIPPI [1] (Graduate Student Member, IEEE)

[1]Department of Electrical and Computer Engineering, Democritus University of Thrace, 67100 Xanthi, Greece
[2]NET2GRID BV, 54630 Thessaloniki, Greece
[3]School of Electrical and Computer Engineering, Aristotle University of Thessaloniki, 54124 Thessaloniki, Greece

CORRESPONDING AUTHOR: T. A. PAPADOPOULOS (thpapad@ee.duth.gr)

This work was supported in part by the Hellenic Foundation for Research and Innovation (HFRI) under the First Call for HFRI Research Projects to Support Faculty Members and Researchers, and in part by the Procurement of High-Cost Research Equipment Grant under Project HFRI-FM17-229.

ABSTRACT The evolution of distribution networks to active systems as a consequence of the increased penetration of distributed energy resources and the electrification of traditionally fuel-based activities have changed drastically the landscape of power systems operation promoting the necessity of benchmarking tools for planning studies. Nevertheless, there is a scarcity of such tools that enable the holistic analysis of modern power systems according to the new grid standards. In this paper, a multi-purpose benchmarking testbed for low-voltage active distribution networks is introduced. The testbed comprises a granular residential appliance-level dataset, a benchmarking framework based on quasi-static simulations, a set of technical indices and a non-intrusive load monitoring tool. A suite of benchmark case studies including overvoltage, undervoltage and line congestion is presented, supported by ancillary trouble-shooting services, such as voltage control and demand response. The proposed testbed can be a useful tool for distribution system operators to evaluate the operating conditions of the grid without violating technical limitations, test new technologies, identify operational challenges, and foresee grid investments.

INDEX TERMS Benchmarking, bottom-up modeling, demand response, distribution network, non-intrusive load monitoring, quasi-static simulations.

I. INTRODUCTION

NOWADAYS, the ever-increasing penetration of distributed renewable energy sources (DRESs), such as photovoltaics (PV) and small wind turbines, into low-voltage (LV) networks gradually transforms the conventional distribution networks (DNs) to active distribution networks (ADNs). Accompanied by a new electrification era that rises through the adoption of power-intensive appliances, such as electric vehicles (EVs) and heat pumps, this inevitable shift towards ADNs poses unprecedented technical challenges to distribution system operators (DSOs) jeopardizing the reliable operation of power systems [1], due to e.g., power fluctuations, voltage violations, and network overloading.

To comprehensively assess the repercussions of the aforementioned problems on the DN performance and to effectively remedy them, systematic studies based on power flow analysis are necessary [2]. Traditional power flow analyses focus on a single snapshot of the power system under certain operating conditions aiming to identify potential voltage or thermal violations. Nevertheless, due to the stochastic variation of loads and the intermittent nature of DRESs, the applicability and effectiveness of the conventional static power flow approach in ADNs is limited, since only major operational conditions at specific time instants can be analysed. To alleviate these constraints, the IEEE Std 1547.7-2013 [2] has defined the quasi-static approach as *"a sequence of steady-state power flow conducted at a time step of no less than 1 s"* by using consumption and generation timeseries as input. By means of quasi-static analysis, the limitations imposed by the stochastic nature of loads and DRESs are effectively addressed.

Besides the need of quasi-static analysis, recent developments in DNs, such as DRESs, battery energy storage (BES) systems, and demand response (DR) mechanisms, dictate the need of new benchmark systems [3]. In the existing literature, LV benchmark networks are passive or present low installed DRES capacity deviating from modern ADNs [4], [5]. Through the prism of facilitating the integration of new technologies, the introduction of benchmark networks incorporating DRESs, BES systems, and DR mechanisms is pivotal.

The motivation of this paper is to create a multipurpose testbed for modern power systems analysis supporting the requirements of grid modernization associated with the integration of DRESs, BES, EVs, DR and novel control schemes. In this context, the ''Bottom-Up Modeling and Power flow analysis (BUMP)'' simulation testbed is introduced, comprising of a granular residential appliance-level dataset, a benchmarking framework, a set of technical indices, and a non-intrusive load monitoring (NILM) tool. According to the authors' knowledge, there is no similar bottom-up testbed in the relevant literature that includes real high-resolution (1 s) appliance-level timeseries data with proper temporospatial diversity [6]. This allows the design, test and analysis of new, flexible and scalable ancillary services and features, e.g., load shifting, voltage regulation schemes, etc.

The core of BUMP is the detailed quasi-static analysis of ADNs and the thorough evaluation of the grid conditions by incorporating high-resolution appliance-level measurements of active and reactive power into the open-source distribution system simulator, OpenDSS [7]. The granular sampling rate enables the support of other services such as near real-time NILM to enable DR strategies. The integrated benchmark framework provides a PV and BES sizing tool and generates scenarios of PV/BES penetration to identify benchmarking test cases, e.g., voltage or thermal violations, in any topology provided by the user. These are of utmost importance and can be used by system operators and academia as reference to test the impact of new technologies and control schemes. In addition, this framework can be a diagnostic tool enabling predictive network maintenance, outage avoidance and investment planning. Additional strengths and contributions of BUMP are:

- Active elements of DNs (PVs and BES) and modern power-intensive loads (EVs and heat pumps) are considered; their impact on the reliable grid operation and potential integration in ancillary services are also investigated.
- Unlike other well-known and publicly available datasets [8], [9], appliance-level reactive power measurements are used for more accurate load modeling to capture the changing trends in the reactive power demand of modern DNs.
- A LV multi-purpose test system is proposed based on the IEEE European LV DN [4]. Modifications have been applied to address cases of modern DNs. The cable ampacities have been provided, allowing operational studies focused on thermal violations which were hindered due to the absence of such information in the original work.
- By means of the benchmarking framework, a suite of benchmark case studies is developed investigating overvoltage, undervoltage, unbalance, and congestion operational aspects. Such operational challenges appear in modern ADNs due to the high penetration of active elements and power-intensive loads in contrast to relevant works focusing on passive DNs [4], [10], [11], [12] or ADNs with limited PV penetration [5], [13].
- To facilitate sound benchmarking and identification of critical assets for planning studies, a set of evaluation metrics [1] is incorporated.
- A NILM model capable of detecting the load status of network end-users is developed and integrated into DR services to support the DN operation under critical conditions.
- Finally, the simulation testbed is shared via a publicly available repository encouraging other users to create new benchmarking cases and test new technologies and control schemes.

II. BUMP ARCHITECTURE

This section introduces BUMP and shortly presents the primary functionalities. BUMP is an open-source toolbox incorporating a dataset of granular appliance-level daily profiles used to model the aggregated consumption of end-users in ADNs. Such a dataset enables i) quasi-static simulations to capture the PV and load stochasticity, and ii) the integration and testing of new DR services. Additionally, BUMP can generate case studies of overvoltage, undervoltage, and line congestion, in any provided DN topology, allowing users to benchmark their solutions and control schemes.

The backbone of BUMP testbed consists of software written in Python. By utilizing object-oriented programming, BUMP can model the load, generation, and storage profiles of multiple LV prosumers forming an ADN. Additionally, by providing the grid topology and line parameters, quasi-static analysis is performed to assess the grid operation and identify benchmarking test cases. This is attained by using OpenDSS software as the main power flow solver. BUMP is generic in terms of supporting any unbalanced three-phase topology provided by the user. The necessary input/output communication is achieved via the filesystem. Furthermore, a pre-trained deep neural network (DNN) is adapted to provide near real-time NILM for DR services. BUMP is modular allowing the user to select specific functionalities, e.g., load modeling, quasi-static analysis, benchmarking and DR. An overview of BUMP including the core components, algorithms, and functionalities is illustrated in Fig. 1. The ''Control schemes'' block refers to any custom-made control mechanism imported by users in the form of Python code. All components are described in detail in the following subsections.

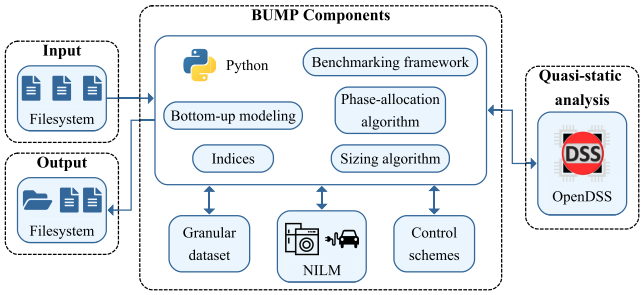

FIGURE 1. BUMP overview.

A. MODELING OF GRID COMPONENTS

The main grid components are residential end-users and solar parks.

1) RESIDENTIAL END-USERS

BUMP simulates residential end-users as potential PV/BES prosumers. In order to model the electricity consumption of each end-user, a bottom-up approach is adopted. The end-user daily demand is generated by aggregating its elementary load components, i.e., individual appliances, by exploiting a high-resolution dataset [14]. The dataset includes daily active and reactive power profiles of commonly used appliances in European houses considering both working (WDs) and non-working days (NWDs). The appliances, their rated power and the number of the available profiles are summarized in Table 1. The dataset is structured as a filesystem directory per appliance containing a file with the active and reactive power timeseries for each available profile. This structure promotes the extensibility of the dataset; a new appliance profile can be easily added by creating the corresponding file in the directory and a new appliance by creating a new directory. BUMP automatically detects the new directories and files, extending the dataset.

BUMP supports both single- and three-phase supplied residential end-users. For single-phase end-users, all appliances and the PV/BES system are connected to the same phase (selected by the user). For three-phase houses, the majority of appliances are single-phase and are allocated to the three phases by applying a greedy algorithm [14] after being sorted in descending order according to their rated power (see Table 1). Finally, EVs, PV and BES systems are considered three-phase symmetrical.

BUMP supports PV systems as the main generation source in LV DNs. To capture multiple stochastic weather conditions such as overcast days, the PVGIS platform [15] was employed to obtain 120 hourly PV generation profiles, 10 for each month of the year. The profiles are normalized at 1 kWp and Akima interpolation [16] was used for upsampling at 1 s. The generation timeseries for each prosumer is derived by multiplying the normalized profile by the installed capacity.

Regarding BES, the adopted control strategy is based on maximizing the self-consumption ratio (SCR) [17]. Under SCR strategy, PV power covers the load demand and any potential surplus of generated power is used for charging. The discharging mode is activated when the PV generation is lower than active power load demand. Additionally, a discrete-time low-pass filter is applied to smooth the charging/discharging power of BES system extending its lifetime expectancy [14].

TABLE 1. Appliances dataset [14].

Appliance	Rated Power [W]	Number of profiles
Air conditioner	1400	30
Dishwasher	2100	18 (WDs) + 3 (NWDs)
Dryer	2300	3
Electric bike	200	30
EV	6600	30
Hair dryer	2100	22
Heat pump	2600	10
Iron	2200	6
Light bulbs (conventional)	200	4
Light bulbs (smart)	60	4
PC	500	39
Range	2200	18
Refrigerator	170	42
Toaster	700	24
TV	108	41
Washing machine	2300	10 (WDs) + 4 (NWDs)
Water heater	4000	6

2) SOLAR PARKS

Apart from residential prosumers, the smart DN can also include small three-phase LV solar parks. Their generation profiles are derived by multiplying their installed capacity with the available normalized PV profiles.

B. DISTRIBUTION NETWORK MODELING

Different network configurations and scenarios can be simulated by adding/removing end-users and modifying their parameters summarized in Table 2. For solar parks, the user can determine the installed capacity and the network node. The network topology is provided via a "*.dss*" file supported by OpenDSS including information for the network frequency, medium-voltage (MV) to LV distribution transformer, and line properties (length, resistance and inductance).

C. BENCHMARKING FRAMEWORK

Quasi-static simulations constitute the cornerstone of BUMP and are conducted via application programming interface (API) calls to OpenDSS. Based on these simulations, the testbed incorporates a scenario-based framework to generate benchmark scenarios addressing undervoltage, overvoltage and/or thermal violations as depicted in Fig. 2. For this purpose, Monte Carlo (MC) simulations are performed to

TABLE 2. Residential end-user parameters.

Demand	number of appliances
	type of appliances
	appliance profiles to be used
Network	single-phase or three-phase power supply
	connected phase in case of single-phase supply
	bus in which the end-user is connected
PV	capacity (PV_{rated})
	profile to be used
BES system	energy capacity (E_{bat})
	maximum permissible power (P_{bat})
	initial state of charge (SoC_{init})
	maximum state of charge (SoC_{max})
	minimum state of charge (SoC_{min})
	charging efficiency (η_{ch})
	discharging efficiency (η_{dch})
	time constant of the low-pass filter (t_{lpf})

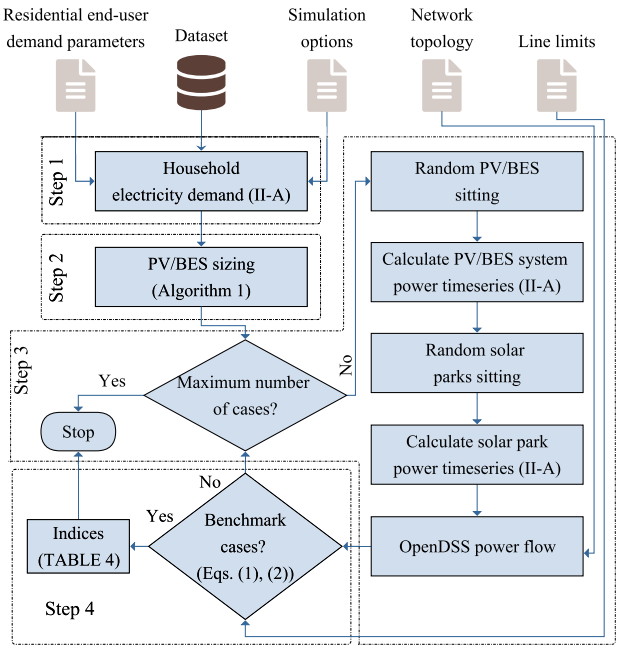

FIGURE 2. Benchmarking framework flowchart.

determine the placement (sizing and sitting) of the PV/BES systems and the solar parks. The proposed benchmarking framework consists of the following steps:

- Step 1: the electricity demand of each household is derived, based on the demand and network parameters of Table 2 determined by the user; for three-phase users the phase-allocation algorithm is applied.
- Step 2: the PV/BES system of each household can be automatically sized by BUMP or determined by the user,
- Step 3: MC quasi-static simulations are performed for the sitting of the PV/BES systems and the solar parks,
- Step 4: benchmark test cases are detected and technical indices are calculated.

In particular, all households are considered as potential prosumers owning a PV/BES system. The PV/BES system size is determined in Step 2 by maximizing the SCR for each household, i. The procedure is summarized in Algorithm 1 and the inputs are presented in Table 3. The outputs are PV^i_{rated}, P^i_{bat} and E^i_{bat}.

TABLE 3. Algorithm inputs and outputs.

Input	Notation
active power timeseries for a single day	$\mathbf{P}^i_{\mathbf{load}}$
1 kWp normalized PV generation profile	$\mathbf{PV}^i_{\mathbf{1kW}}$
BES minimum and maximum permissible power limits in kW	$P^{\min}_{\text{bat}}$, $P^{\max}_{\text{bat}}$
BES minimum and maximum energy capacity limits in kWh	$E^{\min}_{\text{bat}}$, $E^{\max}_{\text{bat}}$
maximum power for single-phase PV systems in kW	$P^{\max}_{\text{PV}-1\text{ph}}$
minimum and maximum power for three-phase PV systems in kW	$P^{\min}_{\text{PV}-3\text{ph}}$, $P^{\max}_{\text{PV}-3\text{ph}}$
ratio $P^i_{\text{bat}}/PV^i_{\text{rated}}$	α
BES maximum C-rate	$C_{\max}$

The algorithm calculates PV^i_{rated} as the ceiling of the total energy consumption of a household (E_{consumed}) over the energy production ($E^{\text{1kW}}_{\text{produced}}$) of the 1 kWp normalized PV profile (PV^i_{1kW}). In Fig. 3, an example of the aforementioned process is presented, depicting the total household consumption and the normalized PV profile, corresponding to E_{consumed} and $E^{\text{1kW}}_{\text{produced}}$. The constraints $PV^i_{\text{rated}} \leq P^{\max}_{\text{PV-1 ph}}$ for single-phase end-users and $P^{\min}_{\text{PV-3 ph}} \leq PV^i_{\text{rated}} \leq P^{\max}_{\text{PV-3 ph}}$ for three-phase end-users are applied; P^i_{bat} is estimated by means of α. In case of low P^i_{bat} or small surplus of generated energy, the BES is considered unnecessary, thus P^i_{bat} (lines 11-12) and E^i_{bat} (lines 17-18) are both set to zero. Eventually, based on $C_{\max}$, the final value of P^i_{bat}, and thus the minimum charging/discharging period, is determined.

Once the sizing algorithm is completed, Step 3 is initiated. BUMP simulates a number of cases by randomly allocating pre-sized PV/BES systems to residential end-users based on two user-defined probabilities p_{PV} and $p_{\text{BES|PV}}$, i.e., the probability for an end-user to be a prosumer (own a PV unit) and the conditional probability of an end-user to own a BES unit, given that is a prosumer. Additionally, a user-defined number of solar parks are randomly allocated to the network; a list of potential buses where solar parks can be placed and their capacity are also provided by the user.

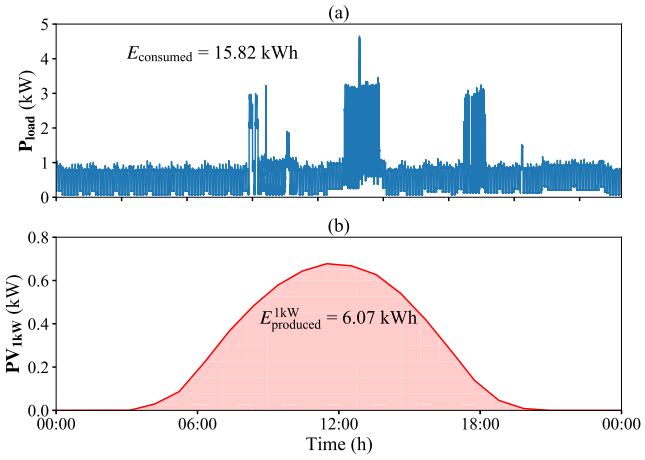

FIGURE 3. Indicative profiles of the (a) total household demand and (b) normalized PV generation.

At each case, 24-h quasi-static simulations are performed to detect benchmarking scenarios. In particular, undervoltage/overvoltage events are identified by comparing the positive-sequence voltage magnitude, V_1, of network buses with the corresponding user-defined thresholds, V_1^{min} and V_1^{max}:

$$\begin{aligned} &\text{undervoltage if } V_1 < V_1^{min}, \\ &\text{overvoltage if } V_1 > V_1^{max}. \end{aligned} \tag{1}$$

For congestion, the line current, I_L, is compared with the cable ampacity limits, I_{amp}:

$$I_L > I_{amp}. \tag{2}$$

Finally, the DN performance is assessed by using a set of end-user- and network-oriented indices described in [1], [18], and [19]; some of the most important indices are summarized in Table 4.

TABLE 4. Most important supported indices.

Index	Description
Current-to-ampacity ratio (ρ)	Occupied capacity of a line
Mean voltage variance (σ^2) [1]	Voltage variations during the day
Losses to load ratio (LLR) [1]	PV/BES effect on power losses
Substation reserve capacity (SRC) [19]	Remaining capacity of the distribution feeder transformer
Voltage level quantification index ($VLQI$) [1]	PV/BES impact on DN voltage level
Voltage unbalance factors (VUF_0, VUF_2) [18]	Severity of voltage unbalance

D. INTEGRATED NILM MODEL

NILM, also known as energy disaggregation, refers to the process of power consumption breakdown on appliance level using the total consumption measurement at the main power service entry [20]. In BUMP, NILM is used to support DR strategies. Due to the ever-increasing energy demand, electric power systems frequently encounter stress conditions and DR has been envisioned to deal with such unexpected conditions by e.g., selectively curtailing system loads and load shifting [21]. By means of DR, the supply-demand equilibrium is preserved increasing the reliability and efficiency of the DN.

Generally, a NILM system can be utilized to identify events of various appliances for residential end-users [22]. Special interest is given on EVs, due to their high power rating, long duration, and charging flexibility that create significant DR potentialities [23] and enable a series of smart services to DSOs. This has motivated the development of a near real-time NILM model for EV detection in BUMP.

The proposed NILM model is based on the recurrent neural network (RNN) described in [24]. The original model performs post-event disaggregation; as the required input is a time window of the total consumption containing the entire target appliance event, disaggregation is performed only after the appliance event is over. In this work, the model has been extended to perform near real-time disaggregation. To that end, although the model architecture has been preserved, the input consists of a sliding non-overlapping window of active power with a length of five minutes (300 samples) and

Algorithm 1 PV and BES Sizing

Input: $P^i_{load}, PV^i_{1kW}, P^{\max}_{\text{bat}}\ P^{\min}_{\text{bat}}\ E^{\max}_{\text{bat}}\ E^{\min}_{\text{bat}}\ P^{\max}_{\text{PV-1 ph}}\ P^{\min}_{\text{PV-3 ph}}$ $P^{\max}_{\text{PV-3 ph}}\ \alpha, C_{\max}$

Output: $PV^i_{\text{rated}}, P^i_{\text{bat}}, E^i_{\text{bat}}$

$T =$ simulation hours
$E_{\text{consumed}} = \text{avg}(P^i_{load}) \cdot T$
$E^{1\text{kW}}_{\text{produced}} = \text{avg}(PV^i_{1kW}) \cdot T$
$PV^{\text{temp}}_{\text{rated}} = \lceil E_{\text{consumed}} / E^{1\text{kW}}_{\text{produced}} \rceil$
if home is single-phase **then**
  $PV^i_{\text{rated}} = \min(PV^{\text{temp}}_{\text{rated}}, P^{\max}_{\text{PV-1 ph}})$
else
  $PV^i_{\text{rated}} = \min(P^{\max}_{\text{PV-3 ph}}, \max(PV^{\text{temp}}_{\text{rated}}, P^{\min}_{\text{PV-3 ph}}))$
end if
$P^i_{\text{bat}} = \lceil \alpha \cdot PV^i_{\text{rated}} \rceil$
if $P^i_{\text{bat}} < P^{\min}_{\text{bat}}$ **then**
  $P^i_{\text{bat}} = 0$
else
  $P^i_{\text{bat}} = \min(P^i_{\text{bat}}, P^{\max}_{\text{bat}})$
end if
Calculate *energy_excess* as the generated energy surplus during hours of PV production
if *energy_excess* $< E^{\min}_{\text{bat}}$ **then**
  $E^i_{\text{bat}} = 0$
else
  $E^i_{\text{bat}} = \min(\lceil energy\_excess \rceil, E^{\max}_{\text{bat}})$
end if
$P^i_{\text{bat}} = \min(P^i_{\text{bat}}, C_{\max} \cdot E^i_{\text{bat}})$
return $PV^i_{\text{rated}}, P^i_{\text{bat}}, E^i_{\text{bat}}$

the output indicates the EV consumption at the end of the window; thus the model estimates the EV power consumption once every five minutes. The model architecture is presented in Fig. 4 and consists of [24]:

- a 1-d convolutional layer [25] including 16 filters with a receptive field of four samples to automatically extract low level temporal features for the time-varying behavior of the input window without user supervision.
- two bidirectional long-short term memory (bi-LSTM) cells [26] to capture the long-term dependency of the consecutive windows without suffering from the vanishing gradient problem [24]. The existence of these cells is important since they present an internal memory of previous inputs in contrast to other kinds of layers which forget the last input vector when a new input is fed to them.
- two fully connected layers [25] as the regression model to map the bi-LSTM output to the EV consumption.

More information about the model architecture and the selected layers can be found in [24]. Additionally, the mathematical formulation of the layers is discussed in [27].

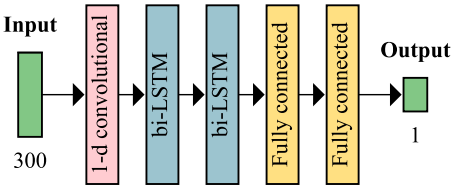

FIGURE 4. Architecture of the NILM model.

In order to train, validate and evaluate the model, three distinct datasets were created. In particular, by using the proposed bottom-up modeling approach, the total consumption timeseries for 14 residential end-users owning an EV were created for seven days; 10 timeseries were used for training, two for validation and two for testing. All timeseries were normalized to speed up learning and achieve a faster convergence. A backpropagation algorithm was used during training to optimize the mean squared error (MSE) between the predicted and the actual EV consumption; Adam optimizer [28] was selected assuming an initial learning rate of 10^{-4}. To avoid over-fitting, early stopping with patience was used; the training process stopped once the validation error did not decrease after three consecutive iterations. Once the training was over, the model was evaluated on the testing dataset and the MSE of the normalized power prediction was $1.5 \cdot 10^{-3}$.

III. BENCHMARK TEST SYSTEM

A. NEED OF BENCHMARK LV TEST SYSTEM

Benchmark systems are standard networks that provide the basis for assessing different technologies and test upon. A number of LV benchmark systems for steady-state analysis can be found in the literature [4], [5], [10], [11], [12], [13]. However, their majority refers to passive network configurations without incorporating DRESs [4], [10], [11], [12]; if done [5], [13] their penetration is limited, being unsuitable to address new challenges encountered in modern DNs. This is further intensified by the increasing number of EV owners. As the EV active power demand is notably higher than other residential appliances, high penetration of EVs is more likely to cause overloading of distribution transformers or other network assets [23]. For such analyses, the knowledge of cable ampacity, i.e., the thermal limits of the network cables, is crucial; however, such information is missing in these test systems [4], [5], [10], [11], [12], [13].

B. ORIGINAL NETWORK

To address the above deficiencies, an enhanced LV benchmark system is proposed based on the IEEE European DN [4]. The IEEE DN is a typical European 50 Hz, three-phase LV feeder of radial structure. It contains 55 single-phase residential loads and is connected to the MV system via a 800 kVA, 11 kV / 0.416 kV delta-wye transformer [29]. Acceptable bus voltages during system operation should be limited in the range 0.9 - 1.1 per-unit (pu) as defined by the Standard EN 50160 [30]. This benchmark topology has been selected as a generalized and representative system for European LV feeders. Nevertheless, it is worth reiterating that BUMP can support any provided topology by the user.

C. CABLE AMPACITY

In the original test system, 10 types of cables are used as backbone and supply cables. Besides the pu-length parameters, cable ampacity is an important cable property for overload and thermal violation studies. Determining the ampacity of each cable is not a trivial task since this information is not readily available in the original datasheet. On the contrary, only the pu-length positive sequence resistance R_1' and inductance X_1' of each cable are provided as summarized in Table 5.

To determine the cable ampacity, an exhaustive review through various datasheets was performed to identify cables with known ampacity corresponding to a similar R_1' and X_1' as the cables of the benchmark system. The resulting cable ampacity is provided in Table 5.

D. ENHANCED NETWORK

The single-line diagram of the proposed test system is shown in Fig. 5. The network topology and cable electrical properties are those of the original test system. Modifications have been applied to the end-users, retaining the network unbalance. Specifically, three-phase end-users have been considered, e.g., at buses 8, 12, 19, etc. Additionally, for some of the single-phase end-users, the connected phase to the power grid has been modified, e.g., bus 55 is connected to phase *a* (originally was connected to phase *c*). Details on the end-users as well as terminal nodes where solar parks can be installed are provided in Fig. 5.

TABLE 5. Cable ampacity.

Name	R_1'	X_1'	Ampacity [A]
2c_.007	3.9700	0.0990	56
2c_.0225	1.2570	0.0850	98
2c_16	1.1500	0.0880	98
35_SAC_XSC	0.8680	0.0920	128
4c_.06	0.4690	0.0750	210
4c_.1	0.2740	0.0730	270
4c_.35	0.0890	0.0675	497
4c_185	0.1660	0.0680	348
4c_70	0.4460	0.0710	210
4c_95_SAC_XC	0.3220	0.0740	233

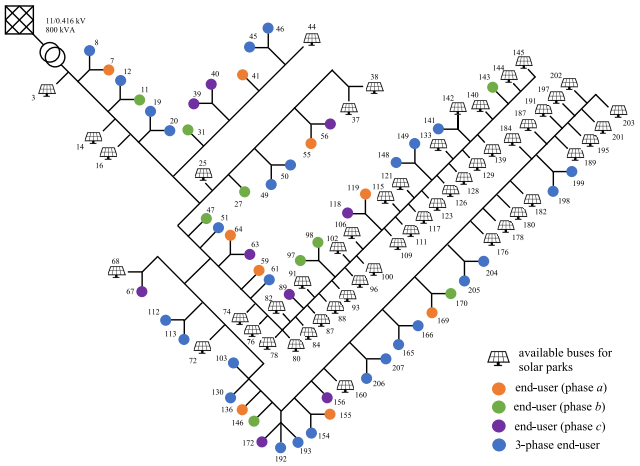

FIGURE 5. Network topology.

IV. CASE STUDIES

By using the enhanced LV test system and the benchmarking framework, three benchmark case studies are proposed investigating scenarios of i) overvoltage, ii) overvoltage and line congestion, and iii) undervoltage and line congestion. The case studies have been selected from a number of 100 MC simulations generated by BUMP assuming high PV, BES, EV, and heat pump penetration. The obtained results are evaluated by using the indices of Table 4 on the basis of the assessment framework of [1]. The mean execution time for a full-day simulation at a resolution of 1 s is 96 min., and the RAM usage is 1,238 MB. Calculations were performed using an Intel Core i7-4790, 3.6 GHz, RAM 8 GB personal computer.

A. BENCHMARK PARAMETERS

For the design of the case studies, first, the electricity demand of each house is derived on the basis of the BUMP dataset and the phase-allocation algorithm. The number and type of appliances were selected considering typical real-world households. For example, common major and small household appliances are the refrigerator and conventional or smart light bulbs. The vast majority of households are equipped with at least one TV and a washing machine. In Fig. 6, the histogram of ownership of each appliance, i.e., the number of residential users owning a specific appliance, is depicted. The validity of the generated demand profiles has been verified via comparisons with findings in the relevant literature in terms of energy. An indicative example is shown in Fig. 3 where the daily energy consumption equals to 15.82 kWh. In particular, the mean daily energy consumption of the generated 29 household profiles without EVs is 12.76 kWh which complies with the mean daily consumption for a four-member family in Germany, i.e., approximately 13 kWh [31].

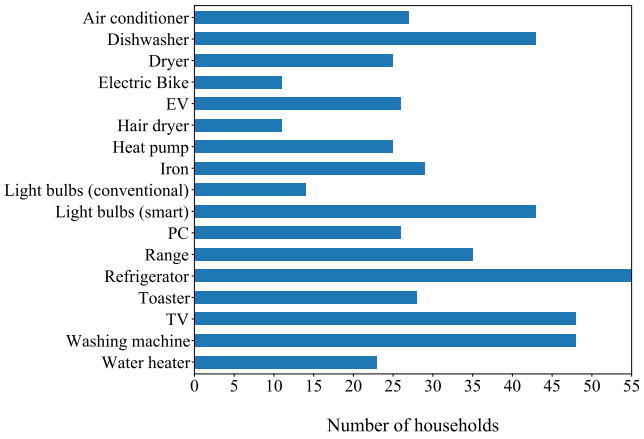

FIGURE 6. Appliance ownership.

Afterwards, the size of the residential PV/BES systems is calculated by applying Algorithm 1. The BES parameters and algorithm inputs are presented in Table 6. A C-rate of two hours, denoted as 0.5C, is assumed meaning that BES can be fully discharged in two hours. Finally, a series of MC quasi-static simulations is performed to determine the PV/BES system and the solar park locations. For all scenarios, p_{PV} and $p_{\mathrm{BES|PV}}$ are taken equal to 70% and 40%, respectively, and a number of eight 20 kW solar parks is used. All converter-interfaced units operate with unity power factor.

B. SCENARIO 1: OVERVOLTAGE

The first scenario is a case of overvoltage caused by high PV penetration and the resulting reverse power flows. The simulated month is July, i.e., when PV production is maximum. The voltage at the secondary of the MV/LV transformer is set to 1.05 pu. The location of PV prosumers, BES and solar parks is summarized in Table 7; the PV/BES size is within the limits of Table 6.

The positive-sequence voltage, V_1, for all buses from 04:00 to 18:00 of the simulated day is illustrated by means of heatmap in Fig. 7. It is evident that during hours of high solar production, i.e., 10:00-14:00, voltage is increased, especially at buses close to the solar parks. The highest voltage is observed at bus 143 at 11:16:50 with a value of 1.11 pu. In this case, no congestion appears as the current is lower than the cable ampacities.

TABLE 6. BES parameters and algorithm inputs.

BES parameters	Value	Algorithm inputs	Value
SoC_{init}	10%	$P_{\text{bat}}^{\max}$	6 (kW)
$SoC_{\max}$	90%	$P_{\text{bat}}^{\min}$	3 (kW)
$SoC_{\min}$	10%	$E_{\text{bat}}^{\max}$	20 (kWh)
η_{ch}	90%	$E_{\text{bat}}^{\min}$	3 (kWh)
η_{dch}	90%	$P_{\text{PV}-1\text{ph}}^{\max}$	5 (kW)
t_{lpf}	100	$P_{\text{PV}-3\text{ph}}^{\min}$	5 (kW)
-	-	$P_{\text{PV}-3\text{ph}}^{\max}$	20 (kW)
-	-	α	0.5
-	-	$C_{\max}$	0.5C

TABLE 7. Scenario 1: PV, BES and solar parks.

Element	Buses
PV	8, 12, 19, 20, 41, 45, 46, 47, 49, 50, 51, 56, 59, 63, 64, 67, 97, 98, 103, 118, 119, 130, 136, 143, 149, 156, 166, 170, 172, 192, 193, 198, 204, 205
BES	12, 20, 41, 50, 59, 97, 103, 149, 166, 192, 205
solar parks	78, 87, 96, 100, 109, 129, 145, 160

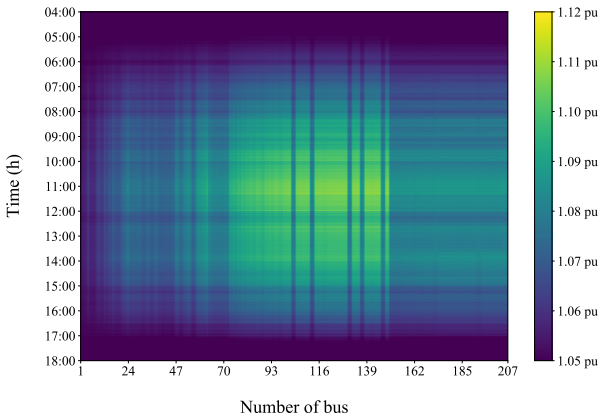

FIGURE 7. Positive-sequence voltage of buses for Scenario 1.

The voltage unbalance caused by the single-phase loads is evaluated by means of the zero- and negative-sequence voltage unbalance factors, VUF_0 and VUF_2, respectively. In Fig. 8 and Fig. 9, the corresponding heatmaps are presented for all buses; the maximum VUF_0 and VUF_2 values are 3.964% and 1.258%, respectively.

To mitigate voltage violations and ensure the reliable operation of the power system, various control schemes have been proposed in the literature [32]. In particular, in LV networks, where a strong dependence between active power and grid voltage exists, the $P(V)$ droop control strategy by curtailing part of the PV injected active power has been

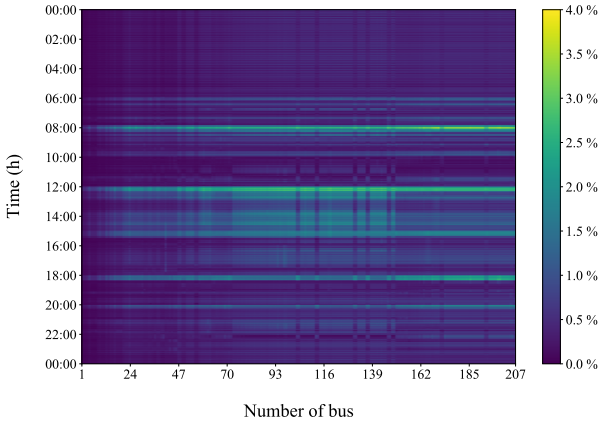

FIGURE 8. VUF_0 heatmap for Scenario 1.

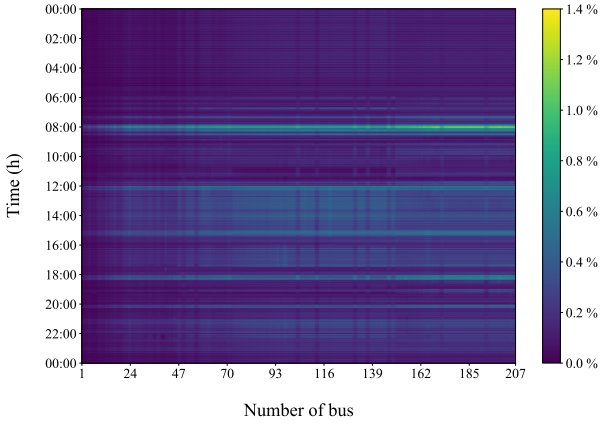

FIGURE 9. VUF_2 heatmap for Scenario 1.

widely-used [33]. The $P(V)$ droop characteristic is depicted in Fig. 10. In this control scheme, the active power of the PV system is adjusted according to the voltage at the point of interconnection (POI) with the grid; P_{MPP} stands for the maximum power point (MPP) that a PV can provide at a specific time instant, and $V_{\text{low}} = 1.09$ pu, $V_{\text{high}} = 1.1$ pu are the voltage thresholds defining the magnitude of the curtailment.

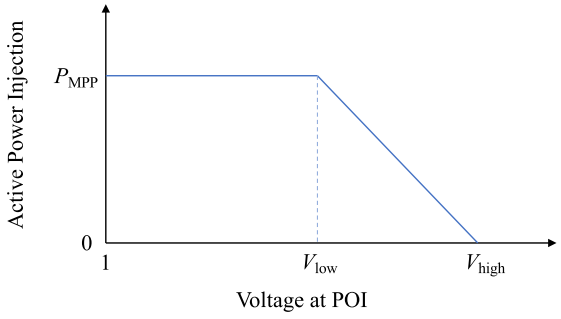

FIGURE 10. Droop characteristic of the $P(V)$ control scheme.

The impact of the droop control on the network voltages can be quantified by means of two network-oriented indices,

namely *VLQI* and σ^2. By applying the droop control scheme, *VLQI* during hours of high solar production and maximum σ^2 have been reduced by 0.36 % and 13.6 %, respectively, compared to the case where no voltage regulation (VR) control is used, indicating reduced network voltages and decreased reverse power flow during high production periods. This is also evident in Fig. 11 where V_1 profile at bus 143, i.e., the bus with the highest overvoltage violation, is compared for the two cases.

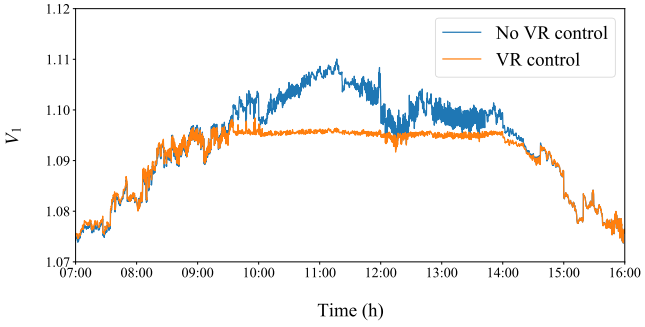

FIGURE 11. V_1 **at bus 143 with and without VR control for Scenario 1.**

C. SCENARIO 2: OVERVOLTAGE AND LINE CONGESTION

In the second scenario, both overvoltage and line congestion are demonstrated. As in the previous scenario, the simulated month is July and the voltage of the secondary of the MV/LV transformer is set to 1.05 pu. The location of PV/BES systems is summarized in Table 8. The maximum V_1 is 1.117 pu at bus 141 at 11:16:50; *VLQI* equals to 1.06255 and the maximum σ^2 is 140.295.

TABLE 8. **Scenario 2: PV, BES and solar parks.**

Element	Buses
PV	7, 8, 19, 20, 31, 45, 46, 50, 56, 59, 61, 97, 98, 112, 113, 118, 119, 136, 141, 143, 146, 148, 149, 154, 155, 165, 166, 169, 170, 172, 192, 198, 199, 204, 206
BES	8, 45, 46, 61, 112, 113, 141, 149, 154, 165, 166, 199, 206
solar parks	87, 88, 106, 115, 123, 128, 133, 202

A heatmap of ρ of phase *a* with respect to time for all network lines is illustrated in Fig. 12. The highest value is observed at line 1 at 09:53:40 and equals 1.068 (the cable ampacity is 210 A and the maximum current 224.28 A). Similar results are also observed for phases *b* and *c*.

In modern DNs, the accurate representation of the power factor is of main importance due to changing trends in reactive power demand. In literature, most analyses focus primarily to active power, assuming a constant power factor for residential end-users. To test this assumption, the power factor of all end-users is calculated. During night and early

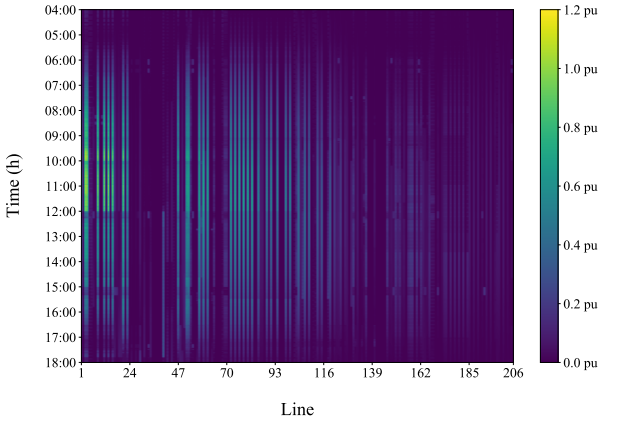

FIGURE 12. **Scenario 2: Heatmap of current-to-ampacity ratio, ρ, for phase *a*.**

morning, when the demand is low and only refrigerators are operating, the power factor is approximately unity. However, during specific periods, e.g., 07:00-09:00, 21:00-22:00, when appliances with operation cycles of low power factor such as dishwashers and washing machines [34] turn on, the power factor decreases to a minimum of 0.932. To investigate the reactive power effect on network operation, *SRC* is calculated assuming both reactive power timeseries (SRC_{Q}) and a standard power factor of 0.95, typically used for residential end-users (SRC_{pf}). The relative percentage difference (*RPD*) [35] between the two cases is calculated as:

$$RPD = 2 \cdot \frac{SRC_{\mathrm{Q}} - SRC_{\mathrm{pf}}}{SRC_{\mathrm{Q}} + SRC_{\mathrm{pf}}} \cdot 100\% \tag{3}$$

and is depicted in Fig. 13 along with SRC_{Q}. Generally, the absolute *RPD* is lower than 1% although there are periods, e.g., 12:00-12:25 and 16:10-18:30, when the difference increases; the highest absolute value is 2.768% appearing at 17:15:50. In addition, the impact of reactive power in network losses is evaluated by means of *LLR*. In the original scenario, *LLR* equals to 0.03853 whereas for a standard power factor the value increases by 3.392%.

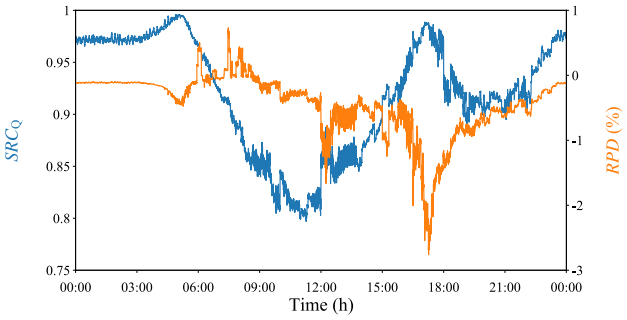

FIGURE 13. SRC_{Q} **and *RPD* for Scenario 2.**

D. SCENARIO 3: UNDERVOLTAGE AND LINE CONGESTION

The aim of this scenario is to demonstrate the ability of a NILM model to provide ancillary services to

DSOs, i.e., enabling DR mechanisms and load-shifting, and, by extension, to support the DN in critical conditions. The violations introduced in this scenario are undervoltage and extreme line congestion due to increased power demand. A higher penetration of EVs is considered to increase network overloading, i.e., 15 additional end-users are assumed to own an EV. The voltage of the secondary of the MV/LV transformer is set to 0.95 pu. The PV/BES system sites are summarized in Table 9.

TABLE 9. Scenario 3: PV, BES and solar parks.

Element	Buses
PV	7, 8, 11, 12, 20, 31, 39, 40, 41, 47, 49, 50, 51, 55, 56, 61, 64, 67, 98, 103, 113, 118, 119, 130, 136, 141, 146, 148, 149, 156, 170, 172, 198, 204
BES	7, 8, 49, 55, 56, 103, 141, 149, 204
solar parks	37, 72, 91, 106, 111, 189, 201, 202

V_1 ranges from 0.893 to 1.004 with the lowest value appearing at bus 205 at 22:05:20; *VLQI* during hours of high solar production equals to 1.07038 and the maximum σ^2 value is 145.123. Additionally, congestion is observed at the network lines. The maximum ρ appears in line 4 (phase c) at 21:03:40 and equals 1.407.

Congestion and undervoltage management is based on the near real-time monitoring of EVs in the DN. The proposed solution includes two steps. During the first step, the NILM model detects in real-time households with EV activity. In this step, disaggregation can be performed either in a decentralized way by integrating the NILM model in the house smart meters [20] or centrally where a cloud platform can receive power measurements from multiple meters. In both cases, the system provides a list of households with EV charging activity to the DSO. In the second step, the DSO can select end-users close to critical nodes and persuade them to shift their charging session during off-peak hours. This can be achieved through DR and monetary incentives, e.g., time-of-use (ToU) rates and decreased cost per kWh [36].

In this scenario, the total demand after 17:00 is very high leading to low V_1 values. The integrated NILM model is used to detect EVs charging after 17:00; overall, 30 EVs are detected. Assuming that seven end-users (located at buses 7, 39, 56, 103, 170, 172, 204) shift their charging session to off-peak hours, i.e., 00:00-08:00, the undervoltage problem is ameliorated leading to a minimum V_1 equal to 0.906 pu and the maximum ρ decreases to 1.145. The total power demand of the DN prior to and after load shifting is presented in Fig. 14. Moreover, in Fig. 15, V_1 at bus 205, where the undervoltage problem was detected, is presented both in the initial scenario and after the load shifting solution.

Finally, it should be noted that by shifting the energy-intensive EVs to off-peak hours, a significant reduction to network losses is achieved; in the original scenario

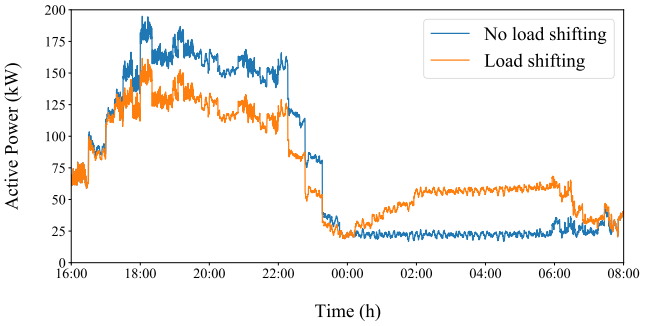

FIGURE 14. Total demand at MV/LV substation with and without load shifting.

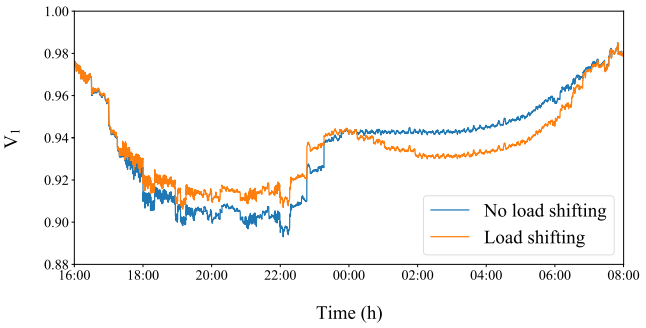

FIGURE 15. V_1 at bus 205 with and without load shifting.

LLR equals to 0.04215 and after load shifting the value drops to 0.03676 resulting in a 12.787% decrease.

V. CONCLUSION

In this paper, a testbed incorporating a granular residential appliance-level dataset, a benchmarking framework, a set of technical indices and a NILM tool is introduced for detailed quasi-static simulations. Given the high penetration of PV/BES systems that DNs will host in the future, the testbed has been used to propose an enhanced version of the IEEE LV DN as well as three benchmark case studies investigating scenarios of i) overvoltage, ii) overvoltage and line congestion, and iii) undervoltage and line congestion.

The proposed testbed can be an ideal tool for DSOs to perform detailed planning studies. By providing the topology of a specific network and allocating DRES/BES units, DSOs can analyse operational challenges encountered in their systems, assess their severity, ensure the reliable operation of the grid without violating technical limitations and test the impact of different technologies, e.g., DR applications, VR and congestion management algorithms. Furthermore, by calculating various technical indices, the most critical assets can be identified allowing DSOs to target their analysis. Finally, the testbed enables DSOs to perform DRES/BES sizing and detect candidate buses for sitting.

Additional data and modeling updates related to harmonic analysis, economic dispatch, protection coordination analysis, transient and dynamic performance studies, etc., will be reported in future BUMP updates.

The Python source code, coding examples and necessary input files for the three test cases are available online https://github.com/christos21/bottom_up.

REFERENCES

[1] K. D. Pippi, T. A. Papadopoulos, and G. C. Kryonidis, "Impact assessment framework of PV-BES systems to active distribution networks," in *Proc. 12th Medit. Conf. Power Gener., Transmiss., Distrib. Energy Convers. (MEDPOWER)*, 2021, pp. 183–189.

[2] *IEEE Guide for Conducting Distribution Impact Studies for Distributed Resource Interconnection*, IEEE Standard 1547.7-2013, pp. 1–137, 2014.

[3] S. H. Dolatabadi, M. Ghorbanian, P. Siano, and N. D. Hatziargyriou, "An enhanced IEEE 33 bus benchmark test system for distribution system studies," *IEEE Trans. Power Syst.*, vol. 36, no. 3, pp. 2565–2572, May 2021.

[4] (Feb. 2017). *Distribution Test Feeders, The IEEE European Low Voltage Test Feeder*. [Online]. Available: https://cmte.ieee.org/pes-testfeeders/resources

[5] K. Strunz et al., "Benchmark systems for network integration of renewable and distributed energy resources," CIGRE, Paris, France, Tech. Rep., TF C6.04.02, Apr. 2014.

[6] F. B. D. Reis, R. Tonkoski, B. P. Bhattarai, and T. M. Hansen, "A real-world test distribution system with appliance-level load data for demand response and transactive energy studies," *IEEE Access*, vol. 9, pp. 149506–149519, 2021.

[7] OpenDSS Program. *Available Through Sourceforge.Net*. Accessed: Dec. 27, 2022. [Online]. Available: http://sourceforge.net/projects/electricdss

[8] J. Kelly and W. Knottenbelt, "The U.K.-DALE dataset, domestic appliance-level electricity demand and whole-house demand from five U.K. Homes," *Sci. Data*, vol. 2, no. 1, pp. 1–14, Mar. 2015, doi: 10.1038/SDATA.2015.7.

[9] J. Kolter and M. Johnson, "REDD: A public data set for energy disaggregation research," *Artif. Intell.*, vol. 25, pp. 1–6, Jan. 2011.

[10] K. Schneider, P. Phanivong, and J.-S. Lacroix, "IEEE 342-node low voltage networked test system," in *Proc. IEEE PES Gen. Meeting Conf. Expo.*, Jul. 2014, pp. 1–5.

[11] R. F. Arritt and R. C. Dugan, "The IEEE 8500-node test feeder," in *Proc. IEEE PES T&D*, Apr. 2010, pp. 1–6.

[12] W. H. Kersting, "Radial distribution test feeders," *IEEE Trans. Power Syst.*, vol. 6, no. 3, pp. 975–985, Aug. 1991.

[13] W. H. Kersting, "A comprehensive distribution test feeder," in *Proc. IEEE PES T&D*, Apr. 2010, pp. 1–4.

[14] G. C. Kryonidis et al., "A bottom-up modelling approach for household power profiles using time-series measurements," in *Proc. 55th Int. Universities Power Eng. Conf. (UPEC)*, 2020, pp. 1–6.

[15] S. Pfenninger and I. Staffell, "Long-term patterns of European PV output using 30 years of validated hourly reanalysis and satellite data," *Energy*, vol. 114, pp. 1251–1265, Nov. 2016.

[16] H. Akima, "A new method of interpolation and smooth curve fitting based on local procedures," *J. ACM*, vol. 17, no. 4, p. 589–602, Oct. 1970.

[17] G. A. Barzegkar-Ntovom, E. O. Kontis, G. C. Kryonidis, A. I. Nousdilis, G. K. Papagiannis, and G. C. Christoforidis, "Performance assessment of electrical storage on prosumers via pilot case studies," in *Proc. 1st Int. Conf. Energy Transition Medit. Area (SyNERGY MED)*, May 2019, pp. 1–6.

[18] E. O. Kontis, G. C. Kryonidis, A. I. Nousdilis, K.-N.-D. Malamaki, and G. K. Papagiannis, "A two-layer control strategy for voltage regulation of active unbalanced LV distribution networks," *Int. J. Electr. Power Energy Syst.*, vol. 111, pp. 216–230, Oct. 2019.

[19] J. Pouladi, T. Abedinzadeh, J. Pouladi, and T. Abedinzadeh, "Performance evaluation of distribution network in presence of plug-in electric vehicles through a new index," in *Proc. 5th Int. Istanbul Smart Grid Cities Congr. Fair (ICSG)*, Apr. 2017, pp. 157–160.

[20] C. L. Athanasiadis, T. A. Papadopoulos, and D. I. Doukas, "Real-time non-intrusive load monitoring: A light-weight and scalable approach," *Energy Buildings*, vol. 253, Dec. 2021, Art. no. 111523.

[21] R. Deng, Z. Yang, M. Chow, and J. Chen, "A survey on demand response in smart grids: Mathematical models and approaches," *IEEE Trans. Ind. Informat.*, vol. 11, no. 3, pp. 570–582, Jun. 2015.

[22] N. Virtsionis-Gkalinikis, C. Nalmpantis, and D. Vrakas, "SAED: Self-attentive energy disaggregation," *Mach. Learn.*, pp. 1–20, Nov. 2021.

[23] J. Wang, G. R. Bharati, S. Paudyal, O. Ceylan, B. P. Bhattarai, and K. S. Myers, "Coordinated electric vehicle charging with reactive power support to distribution grids," *IEEE Trans. Ind. Informat.*, vol. 15, no. 1, pp. 54–63, Jan. 2019.

[24] J. Kelly and W. Knottenbelt, "Neural NILM: Deep neural networks applied to energy disaggregation," in *Proc. 2nd ACM Int. Conf. Embedded Syst. Energy-Efficient Built Environ.*, Jul. 2015, pp. 55–64.

[25] C. Athanasiadis, D. Doukas, T. Papadopoulos, and A. Chrysopoulos, "A scalable real-time non-intrusive load monitoring system for the estimation of household appliance power consumption," *Energies*, vol. 14, no. 3, p. 767, Feb. 2021.

[26] M. Kaselimi, N. Doulamis, A. Doulamis, A. Voulodimos, and E. Protopapadakis, "Bayesian-optimized bidirectional LSTM regression model for non-intrusive load monitoring," in *Proc. IEEE Int. Conf. Acoust., Speech Signal Process. (ICASSP)*, May 2019, pp. 2747–2751.

[27] I. Goodfellow, Y. Bengio, and A. Courville, *Deep Learning*. Cambridge, MA, USA: MIT Press, 2016. [Online]. Available: http://www.deeplearningbook.org

[28] D. P. Kingma and J. Ba, "Adam: A method for stochastic optimization," Jan. 2017, *arXiv:1412.6980*.

[29] A. I. Nousdilis, A. I. Chrysochos, G. K. Papagiannis, and G. C. Christoforidis, "The impact of photovoltaic self-consumption rate on voltage levels in LV distribution grids," in *Proc. 11th IEEE Int. Conf. Compat., Power Electron. Power Eng. (CPE-POWERENG)*, 2017, pp. 650–655.

[30] *Voltage Characteristics of Electricity Supplied by Public Distribution Networks*, Standard EN 50160, 2010.

[31] D. Fischer, A. Hartl, and B. Wille-Haussmann, "Model for electric load profiles with high time resolution for German households," *Energy Buildings*, vol. 92, pp. 170–179, Apr. 2015.

[32] K. D. Pippi, G. C. Kryonidis, and T. A. Papadopoulos, "Methodology for the techno-economic assessment of medium-voltage photovoltaic prosumers under net-metering policy," *IEEE Access*, vol. 9, pp. 60433–60446, 2021.

[33] G. C. Kryonidis, E. O. Kontis, A. I. Chrysochos, C. S. Demoulias, and G. K. Papagiannis, "A coordinated droop control strategy for overvoltage mitigation in active distribution networks," *IEEE Trans. Smart Grid*, vol. 9, no. 5, pp. 5260–5270, Sep. 2018.

[34] M. Pipattanasomporn, M. Kuzlu, S. Rahman, and Y. Teklu, "Load profiles of selected major household appliances and their demand response opportunities," *IEEE Trans. Smart Grids*, vol. 5, no. 2, pp. 742–750, Mar. 2014.

[35] L. Törnqvist, P. Vartia, and Y. O. Vartia, "How should relative changes be measured?" *Amer. Statistician*, vol. 39, no. 1, pp. 43–46, Feb. 1985.

[36] P. Palensky and D. Dietrich, "Demand side management: Demand response, intelligent energy systems, and smart loads," *IEEE Trans. Ind. Informat.*, vol. 7, no. 3, pp. 381–388, Aug. 2011.

CHRISTOS L. ATHANASIADIS (Student Member, IEEE) received the Dipl.Eng. degree from the School of Electrical and Computer Engineering, Aristotle University of Thessaloniki, Greece, in 2019. He is currently pursuing the Ph.D. degree with the Department of Electrical and Computer Engineering, Democritus University of Thrace, Greece. Since 2019, he has been with NET2GRID BV, Thessaloniki, Greece. His research interests include smart meter data analytics, energy disaggregation, and machine learning.

THEOFILOS A. PAPADOPOULOS (Senior Member, IEEE) received the Dipl.Eng. and Ph.D. degrees from the School of Electrical and Computer Engineering, Aristotle University of Thessaloniki, Greece, in 2003 and 2008, respectively.

He is currently an Associate Professor at the Power Systems Laboratory, Department of Electrical and Computer Engineering, Democritus University of Thrace, Greece. His special research interests include power systems modeling, PLC, and computation of electromagnetic transients. He received the Basil Papadias Award from the 2007 IEEE PowerTech Conference. He was also a recipient of the MedPower2020 Best Paper Award and the SEST2022 Best Paper Award.

GEORGIOS C. KRYONIDIS (Member, IEEE) received the Dipl.Eng. and Ph.D. degrees from the School of Electrical and Computer Engineering, Aristotle University of Thessaloniki, Greece, in 2013 and 2018, respectively. Currently, he is an Adjunct Lecturer at the Aristotle University of Thessaloniki. He has an eight years of experience as a researcher in EU Research Projects (FP7, H2020, and Interreg-Med). His research interests include distributed generation and storage, renewable energy sources, microgrids, and smart grids operation and control.

KALLIOPI D. PIPPI (Graduate Student Member, IEEE) was born in Xanthi, Greece, in 1996. She received the degree from the Department of Electrical and Computer Engineering, Democritus University of Thrace, Xanthi, in July 2019, where she is currently pursuing the Ph.D. degree with the Department of Electrical and Computer Engineering.

Her main research interests during her post-graduate studies are related to the ancillary service solutions for transmission and distribution system operators.

Ms. Pippi was a recipient of the MedPower2020 Best Paper Award from the MedPower 2020 Conference.